

# Multimodal Fish Feeding Intensity Assessment in Aquaculture

Meng Cui, Xubo Liu, Haohe Liu, Zhuangzhuang Du, Tao Chen, Guoping Lian, Daoliang Li, Wenwu Wang

**Abstract**—Fish feeding intensity assessment (FFIA) aims to evaluate the intensity change of fish appetite during the feeding process, which is vital in industrial aquaculture applications. The main challenges surrounding FFIA are two-fold. 1) robustness: existing work has mainly leveraged single-modality (e.g., vision, audio) methods, which have a high sensitivity to input noise. 2) efficiency: FFIA models are generally expected to be employed on devices. This presents a challenge in terms of computational efficiency. In this work, we first introduce an audio-visual dataset, called *AV-FFIA*. *AV-FFIA* consists of 27,000 labeled audio and video clips that capture different levels of fish feeding intensity. To our knowledge, *AV-FFIA* is the first large-scale multimodal dataset for FFIA research. Then, we introduce a multi-modal approach for FFIA by leveraging single-modality pre-trained models and modality-fusion methods, with benchmark studies on *AV-FFIA*. Our experimental results indicate that the multi-modal approach substantially outperforms the single-modality based approach, especially in noisy environments. While multimodal approaches provide a performance gain for FFIA, it inherently increases the computational cost, as it require independent single-modality based encoders to process the input data from the individual modalities. To overcome this issue, we further present a novel unified mixed-modality based method for FFIA, termed as *U-FFIA*. *U-FFIA* is a single model capable of processing audio, visual, or audio-visual modalities, by leveraging modality dropout during training and knowledge distillation from single-modality pre-trained models. We demonstrate that *U-FFIA* can achieve performance better than or on par with the state-of-the-art modality-specific FFIA models, with significantly lower computational overhead. Our proposed *U-FFIA* approach enables a more robust and efficient method for FFIA, with the potential to contribute to improved management practices and sustainability in aquaculture. To encourage further research, we release the *AV-FFIA* dataset and the pre-trained model at <https://github.com/FishMaster93/U-FFIA>.

**Index Terms**—Fish feeding intensity assessment (FFIA), computer vision, acoustic technology, audio-visual fusion

## I. INTRODUCTION

**D**IGITAL aquaculture plays an important role in enhancing operational efficiency, sustainability, and productivity in aquaculture [1], [2]. As the foundation of digital aquaculture technology, Fish Feeding Intensity Assessment (FFIA) is the task of evaluating the fish feeding intensity during the feeding process. FFIA offers significant benefits for real-world

Meng Cui, Xubo Liu, Haohe Liu, and Wenwu Wang are with the Centre for Vision, Speech and Signal Processing (CVSSP), University of Surrey, Guildford GU2 7XH, UK. (e-mail: [m.cui, xubo.liu, haohe.liu, w.wang]@surrey.ac.uk).

To Chen, Guoping Lian are with the Department of Chemical and Process Engineering, University of Surrey, Guilford GU2 7XH, UK. (e-mail: [t.chen, g.lian]@surrey.ac.uk).

Zhuangzhuang Du, Daoliang Li are with the National Innovation Center for Digital Fishery, China Agricultural University, China (e-mail: 18437956159@163.com, dliangl@cau.edu.cn).

aquaculture applications by facilitating adjustments to bait dispensing and thereby minimizing feed waste. FFIA serves as a valuable tool for improving productivity in aquaculture [3].

Traditional methods of FFIA primarily rely on the experience of human observers and subjective interpretation [4]. These methods are time-consuming and labour-intensive to operate. With the recent advances in deep learning, data-driven approaches [5]–[16] have become the mainstream methods for FFIA. Existing approaches mainly use digital cameras to capture the corresponding images as input and according to the fish behaviour with discrete feeding intensity (e.g., “None”, “Weak”, “Medium” and “Strong” [14], [17]), characterized as a classification problem modelled by Convolutional Neural Networks (CNNs). However, fish-feeding behaviour is a dynamic and continuous process. Single images are insufficient to capture the context of fish feeding intensity [8]. As an alternative, video-based methods have been proposed to exploit spatial and temporal visual information for FFIA, which offers rich context for capturing fish feeding behaviour. Nevertheless, the processing of video data is computationally demanding, requiring significant computational resources and memory, which makes it impractical for on-device applications that play a crucial role in aquaculture [10]. Furthermore, visual-based methods are highly vulnerable to variations in lighting conditions and noise resulting from water surface reflections [18], [19].

In comparison to visual-based measurements, acoustic measurements present an efficient alternative for FFIA. As acoustic measurements are unaffected by illumination changes and occlusions, they are a reliable solution for round-the-clock 24 hours monitoring. In addition, acoustic data is typically more compact and cost-effective to process compared to raw video data [20], [21]. Cui et al. [22] introduced an audio dataset *AFFIA3K* for FFIA consisting of 3000 labelled audio clips and demonstrated the practicality of audio-based FFIA. Although audio-based models exhibit greater computational efficiency when compared to visual-based models, their performance tends to be comparatively lower. Since audio data lacks the capability to capture the behaviour of fish and physical characteristics compared with visual observation. Furthermore, recorded audio signals are influenced by various underwater acoustic noises, which introduces challenges to learning FFIA from audio data.

The main challenges for FFIA can be categorized into two-fold: 1) Robustness: existing works have mainly relied on single-modality, making them sensitive to input noise; 2) Efficiency: FFIA models are generally expected to be

employed on feeding machines [10], [14]. How to design an accurate and efficient model for FFIA is an ongoing question. 3) Dataset: The limited availability of large-scale multimodal FFIA datasets poses additional challenges in this area.

In this work, we first introduce a large-scale audio-visual dataset for FFIA, called *AV-FFIA*, which comprises 27 000 labelled audio and video clips. To our knowledge, *AV-FFIA* is the first large-scale multimodal dataset for FFIA research. Compared to the existing *AFFIA3K* dataset [22], *AV-FFIA* is approximately 9 times larger and includes video clips corresponding to the audio clips. Despite there are numerous existing research on visual-based FFIA, most of them remain inaccessible. In contrast, our proposed *AV-FFIA* dataset is publicly accessible and much larger.

Human perception of the world is inherently multimodal, while the potential of multimodal FFIA is relatively unexplored. In this work, we introduce an audio-visual approach for FFIA by leveraging single-modality pre-trained models and modality-fusion methods. We conducted extensive benchmark studies on *AV-FFIA*, and experimental results indicate that the multi-modal approach significantly outperforms the single-modal approach, especially in noisy environments. Although the multimodal approach provides more robust performance for FFIA compared with single-modal approaches, it also raises several limitations. For example, the increased computational cost required to process data from multiple modalities simultaneously and the absence of any single modality can degrade the performance of the model.

To achieve a robust and efficient solution for FFIA, we further present a novel unified mixed-modality based approach for FFIA, termed as *U-FFIA*. *U-FFIA* is a single model capable of processing audio, visual or audio-visual modalities, which is achieved by modality dropout to simulate different combinations of input modalities. To achieve an efficient model, we perform preprocessing from the input part of audio and video to reduce redundant information. We first use SimPFs [23] to reduce the redundant information within the mel-spectrogram and use the pre-trained [24] audio models to extract audio features as a complementary modality for helping video with fewer frames. Then, we use the knowledge distillation [25] method, taking a pre-trained model with full audio and video frames as the teacher network, to enhance the performance of the audio and video student network that uses few frames. We demonstrate that *U-FFIA* can achieve performance that is better than or on par with the state-of-the-art modality-specific FFIA models, with significantly lower computational overhead. Furthermore, we conduct extensive experiments on audio, visual, and audio-visual modalities in noisy environments, demonstrating the effectiveness and robustness of our proposed method in various scenarios.

This paper extends our previous work presented at the MLSP 2022 conference [22]. Our contributions can be summarized as follows: (1) We introduce a new large-scale public audio-visual *AV-FFIA* dataset, which is 9 times larger than *AFFIA3K*. We further conduct comprehensive benchmark studies on audio-only and visual-only FFIA models; (2) We propose a new audio-visual approach for FFIA, which significantly improves the robustness of FFIA in noisy environments (e.g.,

audio bubbles noise, visual corruption). Extensive experiments of audio-visual FFIA under different noise conditions are performed to show the efficacy of the proposed method; (3) We introduced a novel unified model, capable of processing both multimodal and single modal input. Our model achieves SOTA performance on *AV-FFIA*, demonstrating its efficacy in noisy environments. Our work is a significant step forward in audio-visual based FFIA.

This paper is organized as follows: The related works about FFIA are described in Section II. Section III introduces audio and video datasets of FFIA that have already been obtained. Section IV describes our benchmark studies on audio, visual and audio-visual fusion based deep learning framework for FFIA. Our proposed novel U-FFIA methods are described in Section V. Experimental details are shown in Section VI. Section VII presents the experimental results and provides an in-depth analysis of the factors contributing to the results. Section VIII concludes the contribution of this paper and discusses the future direction.

## II. RELATED WORK

Feeding is one of the most important variable costs in aquaculture [8]. To overcome the limitations of human-based observation and optimize feeding strategies to reduce costs, many aquaculture factories use automatic feeding machines for fish feeding [6], [14]. However, most feeding machines operate based on fixed thresholds or human experiences, lacking the ability to automatically adjust to fish feeding intensity [10]. FFIA can evaluate the intensity changes in fish appetite during the feeding process and optimize the control strategies of the feeding machine to avoid inadequate feeding or overfeeding, which reduces the feeding cost in industrial aquaculture. Deep learning has the advantages of scalability, adaptability, and robustness, making it widely used in FFIA [7]. In recent years, various deep-learning methods have been used for FFIA. In this section, we provide a summary of related topics and highlight the differences between our work and existing research in FFIA.

### A. Visual-based FFIA methods

As a non-invasive, cost-effective method, computer vision technology has been a popular method for FFIA [18]. In the early step, many researchers use traditional methods (such as background segmentation and target tracking) to assess the fish feeding index [17], [26]. The complex process of foreground segmentation leads to a decrease in computational efficiency and is easily affected by water surface fluctuations, reflective areas, etc [19]. Convolutional neural networks (CNNs) have been widely used in various image recognition tasks, including fish classification [27], counting [28], and tracking [29]. The CNN-based method has also been used in FFIA, e.g., MSIF-MobileNetV3 [7], EfficientNet-B2 [11], offering excellent performance.

The fish feeding behaviour is a dynamic and continuous process that changes rapidly over time. A single image may not reflect the context information of fish feeding behaviour [16]. Videos can capture both spatial and temporal information

on fish feeding behaviour, providing context information for fish feeding behaviour [14], [15]. Converting the original RGB video into an optical flow image sequence and then fed it into a 3D CNN is a common method for video-based FFIA, which outperforms image-based models [12], [14], [30]. However, processing video data is computationally demanding, making it impractical for on-device applications. In addition, uneven illumination and occlusion pose great challenges for video-based FFIA.

### B. Audio-based FFIA methods

Vocalization is an important fish behaviour with approximately 1000 fish species confirmed to produce sounds underwater, and sound signals are usually accompanied by activities such as feeding and reproduction [31], [32]. Fish can make a series of sounds (e.g., splashing sounds, patting tail sounds, swallowing and chewing sounds) during the feeding process, such as the feeding sounds produced by Rainbow Trout (0.02–25 kHz) [33], Japanese Minnow (1–10 kHz) [34], Atlantic horse mackerel (1.6–4 kHz) [35], Yellowtail (4–6 kHz) [36], and Micropterus Salmoide (1–20 KHz) [37]. Fish feeding sounds vary with the intensity of food intake, therefore, we can analyze the fish feeding behaviour through the frequency spectrum of the feeding sound.

The FFIA based on audio was initially proposed by [22], the audio signal is first transformed into acoustic features (i.e., log mel spectrograms) and then fed into a CNN-based model for FFIA. Similar work [38], [39] also demonstrates the feasibility of using audio as model input for FFIA. Compared with vision-based methods, acoustic measurements are more energy-efficient and involve lower computational costs (e.g., energy consumption, data storage cost) [40], [41], which are more suitable for on-device application [23], [42].

Although audio-based models exhibit greater efficiency compared to vision-based models [20], Cui et al., [22] found that their classification performance tends to be comparatively lower than video-based FFIA. On the one hand, audio cannot capture the full information of visually observed fish behaviour, missing visual cues such as body movements or interactions, thereby limiting a comprehensive understanding of fish behaviour. On the other hand, audio signals are sensitive to environmental noise (e.g., pump noise, water flow) and such noise can adversely impact on the detection and analysis of fish vocalizations or other related sounds.

### C. Audio-Visual pattern recognition

Multimodal Pattern recognition (PR) technologies have the advantage of capturing diverse features from different modalities [43]. Audio and visual fusion methods have become increasingly popular methods in PR technologies, which have been successfully applied in numerous fields, including audio-visual event localization [44], [45], audio-visual speech recognition [46], [47], audio-visual emotion recognition [48], [49], and animal behaviour analysis [50]–[54].

A single modality (e.g., audio or visual) can be tailored to suit specific types of data or tasks, requiring fewer computational resources and offering faster processing compared

to multimodal models. However, single modalities have limitations as they provide a restricted perspective on data, considering only one type of input. Consequently, this approach may result in a lack of context and a partial understanding of the overall information. The audio-visual fusion methods can combine different modalities to provide a more comprehensive understanding of the data. In aquaculture, the complementary approach of using video and audio can be better adapted to the challenges brought by various environments. For example, in the case of poor lighting conditions, audio can be used as the main information, and vision is used as auxiliary information.

However, processing multiple modalities simultaneously requires increased computational resources, including memory, processing power, and storage. This can impact system performance and scalability. To address these issues, we focus on the efficient unified model, which can be capable of processing both multimodal and single-modal input. It is worth mentioning that, there is no similar work on the audio-visual fusion method for FFIA, and we are the first to propose the audio-visual fusion method for FFIA. The potential of our proposed approach in aquaculture applications is significant, and it opens up new possibilities for advancing our understanding of FFIA.

## III. DATASET

Although the FFIA plays a crucial role in aquaculture, there is currently no publicly available dataset, which hinders further research and progress in this field. In this paper, we present *AV-FFIA*, a new audio and video dataset comprised of 27 000 labelled fish feeding sound and video clips for FFIA. We will discuss the details in the following sections.

### A. Audio-visual dataset

We used *Oplegnathus punctatus* (a kind of marine fish) as experimental subjects, which were farmed in a recirculating tank with a diameter in 3 meters and a depth in 0.75 meters, located in Yantai, Shandong Province, China. Each fish weighs about 150g. A high-definition digital camera (Hikvision DS-2CD2T87E(D)WD-L) with a frame rate of 25 fps (1920 × 1080) and a high-frequency hydrophone (LST-DH01) with a sampling frequency of 256 kHz were used to collect the fish feeding video and audio data. The acquisition of video data and audio data were carried out at the same time. The high-definition digital camera was deployed on a tripod with a height of about 2 m to capture the video data (as shown in Fig. 1) and a digital hydrophone was used to capture fish feeding audio data underwater. In the process of data collection, we followed the feeding rules in the real aquaculture production environment to ensure that the fish adapts to the laboratory environment as soon as possible and reduces the appetite loss caused by environmental changes. We feed the fish twice a day at 8 am and 5 pm. The video and audio data collection duration is 15 minutes, where the feeding begins in the second minute, and the feeding process lasts about 3–10 minutes. Under the guidance of a fish feeding technician, we annotated the feeding video data as “*Strong*”, “*Medium*”, “*Weak*” and “*None*”. We further divide each one-minute video and audio clip into 30 segments with each segment in two seconds.

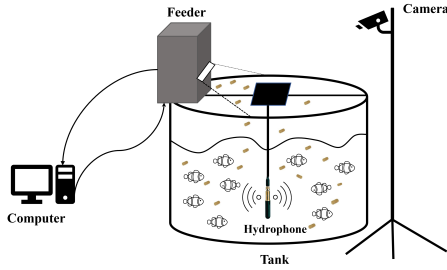


Fig. 1: Experimental systems for data collection. A hydrophone was underwater and the camera was deployed on a tripod with a height of about two meters to capture the video data.

Finally, 27 000 two-second video and audio clips are obtained, namely *AV-FFIA*, with 27 000 video and audio clips for each category of fish feeding intensity. For each class of fish feeding intensity, we create the training, validation and testing set by randomly choosing the audio clips and corresponding video clips. In total, 21 000 clips are used for training, 2800 clips for validation, and 2800 clips for testing.

### B. Visualization of the *AV-FFIA* examples

To enhance the comprehension of diverse fish feeding intensities, we have randomly selected a range of video footage and audio samples to exemplify the varying degrees of fish feeding intensities. Fig. 2 comprises video clips and corresponding audio mel-spectrograms that capture various feeding intensities. The video frames and mel-spectrograms exhibit a well-distributed range of feeding intensities, indicating the high quality of the data. The images demonstrate a direct correlation between the fish hunger intensity and the degree of fish aggregation, with increased hunger intensity leading to a higher level of fish aggregation. Furthermore, the continuous video footage reveals that fish swimming speed and feeding activities are intensified during periods of higher hunger intensity. The corresponding audio clips also exhibit a distinct energy spectrum generated by the fish during their feeding and chewing activities. As the feeding process of the fish concludes, the feeding activity of the fish gradually

decreases, resulting in a return of fish aggregation degree and energy spectrum to normal levels.

## IV. BENCHMARK STUDIES ON *AV-FFIA*

To facilitate the study of the FFIA task, we introduce the *AV-FFIA* dataset and conduct several benchmark studies on audio, visual, and audio-visual fusion modalities. This comprehensive dataset and benchmark provide researchers with a valuable resource to evaluate and compare the performance of different FFIA approaches across various modalities.

### A. Audio-based FFIA

CNN has proven to be highly effective in capturing complex spectral and temporal features, making it a widely-used approach in audio classification tasks, such as bird species classification and frog sounds classification [55]–[57]. We aim to provide valuable insights to future researchers working in the field of FFIA by exploring the most common CNN-based model for our *AV-FFIA*. Recently, large-scale self-supervised pre-trained models have significantly improved the performance of audio classification tasks, giving state-of-the-art performance in this area. For example, PANNs [24] and AST [58] have demonstrated remarkable results on the AudioSet [59]. Therefore, to explore the full potential of our *AV-FFIA* dataset, we leverage the pre-trained models (PANNs, AST) and fine-tune them on our *AV-FFIA* dataset. However, computational complexity is an important issue when systems are implemented on devices, especially in aquaculture. For this purpose, we adopted the MobileNetV2 model proposed in PANNs [24] as our backbone model. The utilization of MobileNetV2 allows us to strike a balance between model performance and computational efficiency in aquaculture applications.

### B. Video-based FFIA

Fish feeding behaviour is a dynamic and ever-changing process, making it challenging to accurately assess the feeding intensity from a single image, especially when distinguishing between subtle differences, such as between fish feeding intensities categories “*Medium*” and “*Weak*”. To address this

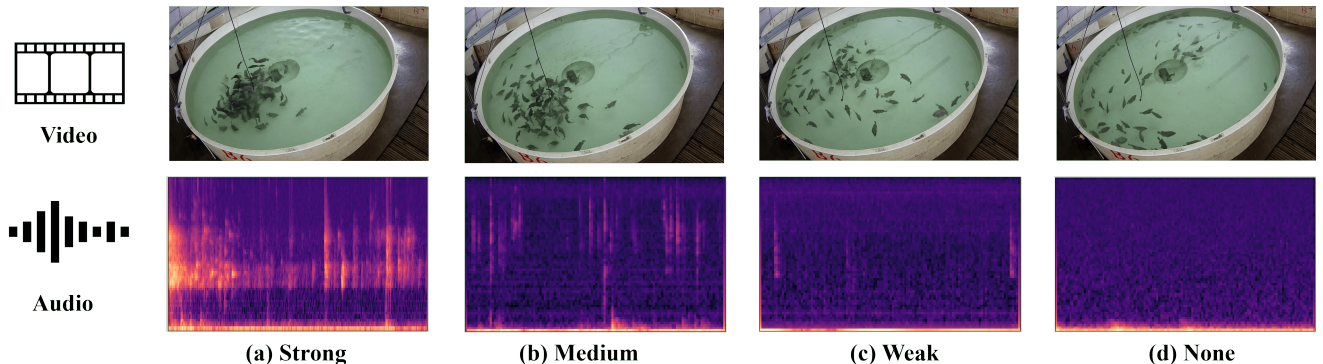


Fig. 2: Video frames and mel spectrogram visualizations of four different fish feeding intensity: “*Strong*”, “*Medium*”, “*Weak*” and “*None*”.

challenge, we leverage the 3D CNNs as our model backbone for video classification. 3D CNNs have proven their effectiveness in various video tasks, such as action recognition [60] and human behaviour analysis [61], making them well-suited for our FFIA task. Notably, state-of-the-art models like I3D [14] and 3D-ResNet [8] have shown promising performance in FFIA, validating the suitability of 3D CNNs for this domain. To provide a robust benchmark study for FFIA, we employ the most common 3D CNNs as our classification model backbone and evaluate their performance on the *AV-FFIA* dataset. Furthermore, in recent advancements, Transformer-based video classification models (e.g., ViViT [62] and 3D-ViT [63]) have demonstrated state-of-the-art results on benchmark datasets like Kinetics-400 and Kinetics-600. We explore the potential of these Transformer-based models on our *AV-FFIA* dataset. By doing so, we aim to gain valuable insights into the suitability of different model architectures for FFIA tasks. However, the processing of video data is computationally demanding, making it impractical for on-device applications. In order to tradeoff video classification performance and model size, we compared the commonly used video classification models and finally chose the Separable 3D CNN (S3D) model [64] as our video classification model. The core idea is to replace the original I3D convolutions [65] with spatial and temporal-separable 3D convolutions. Compared with the I3D model [14], S3D model has greatly reduced the number of model parameters and improved performance on Kinetics (a large-scale human action video dataset). Therefore, we used a pre-trained S3D model on Kinetics and fine-tuned it on the *AV-FFIA* dataset.

### C. Audio-visual fusion FFIA

Although audio and visual-based methods achieved good performance, they still have some limitations, such as the sensitivity to the impact of noise and lack of contextual understanding. The audio-visual fusion method offers the advantage of presenting more comprehensive information for FFIA, which could be highly beneficial in the field of aquaculture. However, existing research on FFIA is limited to single-modality based approaches, which may not fully capture the complexity and dynamics of the feeding behaviour. Hence, we propose several audio-visual fusion methods for FFIA, which allow us to simultaneously capture both the visual and audio cues associated with the feeding behaviour. By leveraging these fusion approaches, we conducted extensive benchmark studies on *AV-FFIA* and gained a deeper understanding of fish feeding behaviour in aquaculture. In this section, we present several audio-visual fusion methods and study the performance of these methods on the *AV-FFIA* dataset.

1) *Audio-visual fusion via multi-head self-attention*: The *multi-head self-attention* fusion method is a straightforward and powerful approach that leverages the regular transformer [66] for processing multimodal inputs. The method involves independently splitting each frame and mel-spectrogram, following the encoding approach proposed in ViT [67]. By concatenating the audio and video tokens, a new sequence of tokens is formed. These concatenated tokens are then used as

the input for the multi-head attention (MHA) module, which can be formulated as follows:

$$\text{MHA}(\mathbf{Q}, \mathbf{K}, \mathbf{V}) = \text{Softmax}\left(\frac{\mathbf{Q}\mathbf{K}^\top}{\sqrt{d}}\right)\mathbf{V}, \quad (1)$$

where  $\mathbf{Q}, \mathbf{K}, \mathbf{V}$  are the query, key, and value matrices obtained using learnable projection weights  $\mathbf{W}^Q, \mathbf{W}^K, \mathbf{W}^V \in \mathbb{R}^{d \times d}$  respectively.

2) *Audio-visual fusion via multi-head cross-attention*: Cross-attention allows for the integration of both audio and visual information, leveraging the strengths of each modality. By fusing information from multiple modalities, the performance can be significantly improved compared to using a single modality alone. The operation can be written as:

$$\mathbf{O}^{(\ell)} = \text{MHA}\left(\mathbf{V}^{(\ell-1)}, \mathbf{A}^{(\ell-1)}, \mathbf{A}^{(\ell-1)}\right) \quad (2)$$

where  $\mathbf{V}^{(\ell-1)}$  is a visual patch representation at layer  $\ell - 1$ , and the  $\mathbf{A}^{(\ell-1)}$  is the audio patch representation. The matrix  $\mathbf{Q}$  is obtained using learnable projection weights from video, while  $\mathbf{K}$  and  $\mathbf{V}$  are obtained using learnable projection weights from audio. Then, we use the Multi-Head Cross-Attention to calculate the new audio-visual fused representation  $\mathbf{O}^{(\ell)}$  as a weighted summation of the audio-visual features.

3) *Fusion via attention bottlenecks*: Bottleneck attention [68] is a technique used in multimodal fusion to address the problem of attention bottlenecks, which can occur when the number of modalities or the dimensionality of the feature space is large. It can be represented as follows:

$$\mathbf{z}_{\text{fsn}} = [z_{\text{fsn}}^1, z_{\text{fsn}}^2, \dots, z_{\text{fsn}}^B] \quad (3)$$

where  $\mathbf{z}_{\text{fsn}}$  means a small set of  $B$  fusion bottleneck tokens.

We then restrict all cross-modal attention flow via these bottleneck tokens. More formally, for layer  $l$ , we compute the token representations as follows:

$$\left[\mathbf{z}_{\text{rgb}}^{l+1} \parallel \hat{\mathbf{z}}_{\text{fsn}}^{l+1}\right] = \text{Transformer}\left(\left[\mathbf{z}_{\text{rgb}}^l \parallel \mathbf{z}_{\text{fsn}}^l\right]; \theta_{\text{rgb}}\right) \quad (4)$$

$$\left[\mathbf{z}_{\text{spec}}^{l+1} \parallel \hat{\mathbf{z}}_{\text{fsn}}^{l+1}\right] = \text{Transformer}\left(\left[\mathbf{z}_{\text{spec}}^l \parallel \mathbf{z}_{\text{fsn}}^l\right]; \theta_{\text{spec}}\right)$$

$$\mathbf{z}_{\text{fsn}}^{l+1} = \text{Avg}_i\left(\hat{\mathbf{z}}_{\text{fsn}_i}^{l+1}\right) \quad (5)$$

where  $i$  indexes each modality, *Transformer* is the Transformer encoder,  $\mathbf{Z}_{\text{rgb}}$  is video tokens and the  $\mathbf{Z}_{\text{spec}}$  is audio spectrogram tokens,  $\left[\mathbf{z}_{\text{rgb}}^l \parallel \mathbf{z}_{\text{fsn}}^l\right]$  is the concatenation of the audio and video tokens,  $\theta_{\text{rgb}}$  and  $\theta_{\text{spec}}$  is video and audio parameters via the cross-transformer. In this case, the audio and video tokens can only exchange information via the bottleneck token  $\mathbf{z}_{\text{fsn}}$  within a transformer layer. We first create modality specific temporary bottleneck fusion tokens  $\hat{\mathbf{z}}_{\text{fsn}_i}$ , which are updated separately and simultaneously with audio and visual information. The final fused tokens from each cross-modal update are then averaged in Equation (5).

### D. Robustness of FFIA to acoustic and visual noise

Fish behaviour is influenced by various environmental factors, including natural ambient noise and visual disturbances. Incorporating audio-visual noise in fish behaviour analysis

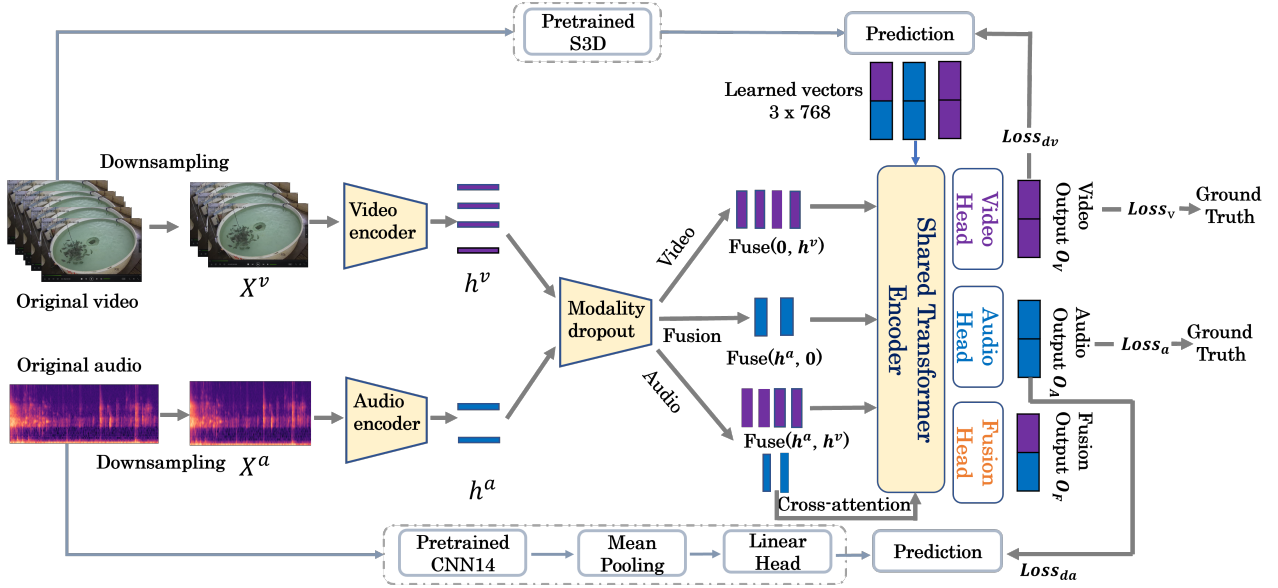


Fig. 3: Overview of the proposed method. We first use the pre-trained video encoder and audio encoder to extract the video and audio features. The audio encoder is a pre-trained PANNs (Pre-trained MobileNetv2 models on Audioset). The video encoder is simply a linear projection layer. We cut the features into non-overlap patches  $16 \times 16$ , and use a modality dropout to randomly select one modality on each step during the model training. The shared transformer encoder has 6 layers with 8 heads, embedding dimension 768, and FFN dimension 1024, using the pre-norm residual connection setup.

helps improve the robustness of the models. For the audio input corruption, we injected a bubble and pump noise to the entire audio with different Signal-to-Noise Ratio (SNR) levels, -10 to 20 dB. For visual input corruption, there can be various noise types, additive noise, blur, colour distortion, occlusion, etc. We use the occlusion and Gaussian noise, that often occurs in actual aquaculture. For the audio-visual input corruption, both audio corruption and visual corruption are injected for random chunks of each stream so that both streams can be corrupted simultaneously or alternatively.

## V. UNIFIED MIXED-MODALITY BASED FFIA

The audio-visual fusion method has demonstrated a notable advantage over the single-modality based approaches, exhibiting robust performance for FFIA even in noisy environments (as shown in our experiments later). However, the need for customizing individual models for each modality has led to increased computational costs, and the absence of any single modality has negatively impacted the overall performance of the audio-visual fusion model. These factors pose significant challenges for FFIA tasks. To address these issues and design an efficient and robust solution for FFIA, we propose a novel unified mixed model, named *U-FFIA*. It is a single model capable of processing audio, visual or audio-visual modalities, which is achieved by modality dropout to simulate different combinations of input modalities. Although there are already existing audio-visual unified models, such as UAVM [69] for VGGSound classification and U-HUBERT [70] for audio-visual speech, these methods are unsupervised methods and demand a substantial volume of unlabeled data for pre-training. Additionally, the training process is intricate

and computationally expensive, which may limit their practical applicability in the context of aquaculture. In contrast, our proposed model employs a supervised training approach and incorporates several innovative techniques to enhance its portability and performance. For example, we address the computational burden arising from temporally redundant audio features, such as mel-spectrograms, by utilizing SimPFs [23] to reduce redundant information. Furthermore, we leverage pre-trained audio models to extract audio features as a complementary modality for helping video with fewer frames. To enhance the performance of the audio and video student networks, we employ knowledge distillation, using a pre-trained model with full audio and video frames as the teacher network. In addition, we conduct extensive experiments on audio, visual, and audio-visual modalities in noisy environments, which demonstrate the effectiveness and robustness of our proposed method in various scenarios. The framework of our proposed model is shown in Fig. 3.

### A. Audio-visual input

We first use the audio pre-processing method to obtain the Mel spectrogram features of the audio signal. However, in the aquaculture environment, various sources of noise, such as bubbles and machine noise, can introduce redundancy in the mel-spectrogram data when used as input to CNNs. To tackle this issue and optimize computational efficiency, we adopt the simple pooling front-ends (SimPFs) [23], [71] method. This technique effectively reduces redundant information present in the input mel-spectrograms, thereby enhancing the overall computational efficiency of the model. The spectral pooling method of SimPF, which computes the discrete Fourier transform (DFT) of the audio frames  $\mathbf{F}^a$  and then crops the centre

with a bounding box with the shape of  $(S, kN^a)$  where  $S$  refers to the dimension of the spectral feature to get  $\tilde{\mathbf{F}}_{\text{crop}}^a$ ,  $k$  denotes the compression rate, ranging from 0 to 1.  $N^a$  is the audio frames. Then the output of the inverse discrete Fourier transform (IDFT)  $\hat{\mathbf{F}}^a$  is taken as the compressed audio, as follows,

$$\begin{aligned}\tilde{\mathbf{F}}^a &= \text{DFT}(\mathbf{F}^a) \\ \tilde{\mathbf{F}}_{\text{crop}}^a &= \mathbf{F}^a(S, kN^a) \\ \hat{\mathbf{F}}^a &= \text{IDFT}\left(\tilde{\mathbf{F}}_{\text{crop}}^a\right)\end{aligned}\quad (6)$$

In order to prevent the model from over-reliance on the video stream, we use the linear layer to encode the video input to force the video encoder to learn simple features and then split each frame following the encoding proposed in ViT. We use the pre-trained MobileNetV2 model as the audio encoder to extract the high-dimensional features of the input Mel spectrogram. Finally, we got the audio input  $h^a \in \mathbb{R}^{T_a \times d}$  and the video input  $h^v \in \mathbb{R}^{T_v \times d}$ , where  $T_a$  is the number of audio features,  $T_v$  is the number of video features and  $d$  is the dimension of the features.

### B. Fusion via efficient video with audio encoding

Compared with the audio input, the video stream is three-dimensional (two spatial and one temporal) and contains a wealth of contextual and temporal information. However, the video contains high redundancy across multiple frames, which makes it computationally expensive to process [72].

We propose an efficient audio-visual fusion framework that uses audio cues for long-range video processing, which reduces the computational cost. For the video modality, we randomly downsample the video frames from the whole input video (50 frames) and get the video input of  $X^v \in \mathbb{R}^{N_f \times 3 \times H \times W}$ , where  $N_f$  is the number of frames,  $H$  is the height of the frame, and  $W$  is the width of the frame. Following the ViT, we split each frame into  $N$  no-overlapping patches, whose shape is  $P \times P$ , and flatten those patches into sequences  $X_p \in \mathbb{R}^{N \times 3P^2}$ . The position embedding is added to the patch embedding to retain positional information. A specialized CLS token  $\mathbf{V}_{cl}^{(0)}$  is prepended to the embedded patches. Finally, the sequences of embedding vectors serve as input to the model as  $\mathbf{h}^v \in \mathbb{R}^{T_v \times d}$ . For the audio modality, we use the pre-trained audio model MobileNetV2 (pre-trained on AudioSet) as the audio encoder to extract the preprocessed mel spectrogram by the SimPFs and then we get the audio features. Afterwards, an average pooling is applied along the frequency dimension and then maximum and average operations are used along the time dimension. We sum the maximized and averaged features and then project them into the shared embedding space through a new multi-layer perception (MLP) block with two linear layers and a ReLU activation hidden layer. Finally, we got the audio embedding  $\mathbf{h}^a \in \mathbb{R}^{T_a \times d}$ . We also prepend the specialized audio class token  $\mathbf{A}_{cl}^{(0)} \in \mathbb{R}^{1 \times 768}$  to the audio-embedded patches.

To efficiently incorporate temporal audio cues into static video frame representations to help reduce the computational

cost of video frames, we use an audio-to-video attention algorithm. This method can be written as:

$$\mathbf{S}_t^{(\ell)} = \text{MHA}\left(\mathbf{V}_t^{(\ell-1)}, \mathbf{V}_t^{(\ell-1)}, \mathbf{V}_t^{(\ell-1)}\right) + \mathbf{V}_t^{(\ell-1)} \quad (7)$$

$$\mathbf{O}_t^{(\ell)} = \text{MHA}\left(\mathbf{S}_t^{(\ell-1)}, \mathbf{A}^{(\ell-1)}, \mathbf{A}^{(\ell-1)}\right) + \mathbf{S}_t^{(\ell-1)} \quad (8)$$

where  $\mathbf{V}_t^{(\ell-1)}$  is a visual patch representation, and  $\mathbf{S}_t^{(\ell)} \in \mathbb{R}^{(N+1) \times d}$  is the newly computed video representation,  $\mathbf{A}^{(\ell-1)} \in \mathbb{R}^{t \times d}$  is the audio representation at layer  $l-1$ , and  $\mathbf{S}_t^{(\ell-1)} \in \mathbb{R}^{(N+1) \times d}$  is the video representation at layer  $l-1$ . To calculate the new audio-visual representation  $\mathbf{O}_t^{(\ell)}$ , we utilize the Multi-Head Cross-Attention mechanism, which performs a weighted summation of the audio-visual features. This allows the model to effectively incorporate long-range audio cues into the visual features. Due to the compact nature of the audio representation, this operation can be efficiently implemented.

We perform temporal pooling over the CLS tokens  $\mathbf{AV}_{cl}^{(0)}$  across all video frames, resulting in the final audio-visual representation  $\mathbf{f} \in \mathbb{R}^d$ . To produce the final output embedding vector, three different learnable CLS tokens are employed. During training, the classification head is implemented using three MLPs with one hidden layer. This decoding strategy enables the model to produce multiple outputs as required, making it suitable for dense tasks like knowledge distillation or contrastive learning.

### C. Modality dropout

In the context of multi-modal learning scenarios, it is common to encounter situations where one or more modalities may be absent or unavailable. For example, in tasks involving multi-modal recognition, certain videos may lack accompanying audio or textual information. To address this challenge, we develop a method called ‘‘modality dropout’’, motivated by the work in [73]. More specifically, this approach is designed to train the model in such a way that it can effectively handle missing modalities by randomly excluding specific modalities during the training process. With this method, the model can be prevented from over-relying on a particular modality, such as audio, which may lead to the neglect of valuable information from other modalities, like video. The modality dropout encourages the model to produce predictions irrespective of the modalities used as input, thereby enhancing its overall robustness. In this study, we adopt modality dropout to prompt the model to learn how to optimally utilize the available modalities while handling instances where certain modalities are missing. As a result of training with modality dropout, the model becomes proficient in leveraging the available modalities effectively, even when some modalities are not present. This approach is shown to improve performance and enhance robustness, as shown in our experiments. Moreover, our approach is capable of making predictions for three distinct input modalities using a single model. This simplifies the hyperparameter selection process and improves computational

efficiency, which is highly promising for applications in aquaculture.

In this study, we employ modality dropout as a technique to mask the complete features of one modality before fusing the audio and visual inputs into the transformer encoder. When both audio and video modalities are utilized as inputs, we assign a probability of  $p_{av}$  for their joint selection. Conversely, when only one modality is used, the audio input is selected with a probability of  $p_a$ , while the video input is selected with a probability of  $1 - p_a$ . The feature fusion process with modality dropout is mathematically represented as follows:

$$\mathbf{f}_t^{av} = \begin{cases} \text{concat}(\mathbf{f}_t^a, \mathbf{f}_t^v) & \text{with } p_{av} \\ \text{concat}(\mathbf{f}_t^a, \mathbf{0}) & \text{with } (1 - p_{av})p_a \\ \text{concat}(\mathbf{0}, \mathbf{f}_t^v) & \text{with } (1 - p_{av})(1 - p_a) \end{cases} \quad (9)$$

where concat means the channel-wise concatenation. We use the modality dropout at each iteration during the self-training.

#### D. Unified model with knowledge distillation

Since we employ a limited number of frames for both audio and visual inputs and a single model to train three modalities, there is a possibility that the performance might be comparatively lower than that of a customized single-modality based model. To address this limitation, we leverage the technique of knowledge distillation (KD) to enhance the performance of our audio and visual models. Knowledge distillation, initially proposed by Hinton et al. (2015) [25], is a model compression method wherein a large-scale model (Teacher) is compressed into a smaller model (Student) while preserving similar performance. This compression process results in improved inference speed, making it more convenient for practical industrial applications [74]. The essence of knowledge distillation is using the logits output by the teacher model (in this case, the pre-trained audio model, CNN14, and visual model, S3D) as the supervision information to guide the learning of the smaller student model and the teacher model uses all the audio and visual frames. During training, we freeze the teacher model to focus solely on training the student model using the knowledge distillation loss. By employing knowledge distillation, we effectively transfer the knowledge learned by the larger teacher model to the compact student model. This approach empowers the student model to achieve enhanced performance, thereby rendering it suitable for practical applications, particularly in domains such as aquaculture. We use the following loss for the student model training:

$$\text{Loss} = \lambda \text{Loss}_g(\psi(Z_s), y) + (1 - \lambda) \text{Loss}_d(\psi(Z_s), \psi(Z_t/\tau)) \quad (10)$$

where  $\lambda$  is the balancing coefficient,  $y$  is the ground truth of FFIA,  $\text{Loss}_g$  and  $\text{Loss}_d$  are the ground truth and distillation losses, respectively,  $\psi$  is the activation function,  $Z_s$  and  $Z_t$  are the logits of the student and teacher model, respectively, and  $\tau$  is the temperature parameter. In this paper, we use the Kullback-Leibler divergence as  $\text{Loss}_d$ . For cross-model KD, the teacher and student may have different logit distributions,

thus we only apply  $\tau$  on the teacher logits to explicitly control the difference.

## VI. EXPERIMENTS

### A. Audio data preparation

1) *Audio data processing*: We use mel spectrogram as acoustic features, which has been widely used for audio classification [24]. The original audio sampling rate is 256 KHz, which can lead to computational and storage burdens. We down-sample the audio signals to 64 kHz to reduce the computational complexity. Then we calculate the Short-Time Fourier Transform (STFT) with a Hanning window of 2048 samples and a hop size of 1024 samples, and finally, we apply the mel filter banks with 128 bins. Therefore, for a 2-second audio signal, we have a mel spectrogram with the shape of  $128 \times 128$ . We use the SimPF method which is a simple non-parametric pooling operation, to reduce the redundant information within the mel-spectrogram, leading to a shape of  $64 \times 128$  mel spectrogram. This streamlined mel spectrogram representation enhances the efficacy of audio classification tasks. To evaluate the noise robustness of the model, we add a bubble and pump noise to the entire audio with different SNR levels, -10 to 20 dB.

2) *Loss and training*: During training, we use the SpecAugment method proposed in [75] to expand our training samples. With SpecAugment, the spectrogram can be modified by masking blocks of consecutive frequency channels, and masking blocks of time steps [75]. Frequency masking is applied such that  $f$  consecutive mel frequency bins  $[f_0, f_0 + f]$  are masked, where  $f$  is chosen from 0 to a frequency mask parameter  $f'$  in terms of a uniform distribution, and  $f_0$  is chosen from  $[0, F - f]$ , where  $F$  is the number of mel frequency bins [76]. The cross-entropy loss is particularly well-suited for classification problems. This loss function quantifies the dissimilarity between the predicted class probabilities and the ground truth class labels. By choosing the cross-entropy loss, we can effectively train our model to improve its classification performance.

### B. Video data processing

The original video comprises 50 frames, each with a resolution of  $2560 \times 1440$ , resulting in a substantial amount of redundant information across multiple frames. To address this issue and reduce computational complexity, we employ a downsampling technique. Specifically, we randomly select 4 frames from the video and resize each frame to a smaller dimension of  $224 \times 224$ . This resizing step aims to retain essential visual information while making the data more manageable for training purposes. By combining downsampling, random cropping, and colour augmentation techniques during training, we effectively utilize the high-resolution video data while promoting the model's ability to generalize well to diverse inputs. For visual noise corruption modelling, we add darkness and Gaussian noise with a maximum variance of 0.2.



### C. Experimental setups

1) *Audio experiment setup*: We use the pre-trained MobileNetV2 models on Audioset and fine-tune it on the AV-FFIA dataset. The Adam optimizer [77] with a learning rate of 0.001 is used for training the model. The batch size is set to 200 and the number of epochs is 20. The training and evaluation are performed on a Nvidia-RTX-3090Ti-24GB GPU.

2) *Video experiment setup*: We use a pre-trained S3D model [64] on Kinetics, and fine-tuning it on our AV-FFIA dataset. We use Adam optimizer with a learning rate of 0.001 for fine-tuning the model. The batch size is set to 20 and the number of epochs is 20. The training and evaluation are performed on a Nvidia-RTX-3090Ti-24GB GPU.

3) *Audio-visual fusion setup*: We use the pre-trained MobileNetV2 model and S3D model to extract the audio and video features, respectively. Then, we split the audio and visual features following the encoding proposed in ViT. We use the ViT architecture ( $L = 6$ ,  $N_H = 8$ ,  $d = 1024$ ) as our backbone. We trained the model on the AV-FFIA Train data and evaluated them on the AV-FFIA Test data. The model is trained on Nvidia-RTX-3090Ti-24GB GPU with a batch size of 20, the number of epochs 200, and the Adam optimizer with a learning rate of 0.0001.

4) *Unified mixed-model setup*: We use the pre-trained MobileNetV2 model to extract audio features and use an average pooling along the frequency dimension. For the video, we use the linear layer to encode the video input into simple features and then split each frame following the encoding proposed in ViT. We also use the ViT architecture ( $L = 6$ ,  $N_H = 8$ ,  $d = 1024$ ) as our backbone. We use Adam optimizer with a learning rate of 0.0001 for training the model. The batch size is set to 20 and the number of epochs is 400. For Knowledge distillation during the training, we fix the hyperparameters  $\lambda = 0.5$  and  $\tau = 2.5$ , which control the balance between the teacher and student models' contributions and the temperature of the softened probabilities, respectively. We use the cross-entropy (CE) loss as  $Loss_g$  and the softmax activation function during training. The training and evaluation are performed on a Nvidia-RTX-3090Ti-24GB GPU.

### D. Evaluation metrics

Accuracy refers to the number of correct predictions divided by the total number of predictions, which provides a straightforward and intuitive measure of the overall performance of a classification model. In most of the literature on the classification of FFIA, accuracy is a popular evaluation metric for classification. In order to compare with the methods in the previous literature, we also use accuracy as the performance metric in our evaluations.

## VII. RESULTS AND DISCUSSION

### A. The benchmark results of audio-based FFIA

We conducted an extensive evaluation of various common methods for FFIA on our AV-FFIA dataset, including CNN, ResNet, and MobileNet models. The performance of these baseline models on the AV-FFIA dataset is presented in Table

TABLE I: The results of the different methods on the AV-FFIA. The FLOPs are computed for one 2-second audio clip with a 64 kHz sampling rate.

Model	Accuracy	Parameters (M)	FLOPs
MobileNetV1	0.823	4.3	198.275
MobileNetV2	0.824	3.5	<b>118.553M</b>
MobileViT	0.794	2.3	229.910M
ResNet18	0.812	39.5	2.676G
ResNet22	0.818	62.6	3.605G
CNN6	0.823	4.6	2.551G
CNN10	0.832	5.0	3.347G
CNN14	0.856	79.7	5.164G
Pre-AST	0.736	85.3	12.440G
PANNs(CNN6)	0.847	4.6	2.551G
PANNs(CNN10)	<b>0.859</b>	5.0	3.347G
<b>MobileNetV2-PANNs</b>	<b>0.857</b>	<b>1.9</b>	<b>133.958M</b>

TABLE II: The video results of the different methods on the AV-FFIA dataset. The FLOPs are computed for one 2-second video clip with 20 frames randomly chosen.

Models	Accuracy	Parameters (M)	FLOPs (G)
I3D	0.791	12.3	35.054
3D-ResNet10	0.855	14.4	28.602
3D-ResNet18	0.874	33.2	42.219
3D-ViT	0.882	27.8	77.614
ViViT	0.743	78.2	77.344
S3D	0.816	7.9	22.826
<b>Pretrained S3D</b>	<b>0.898</b>	<b>7.9</b>	<b>22.826</b>

I. Notably, the CNN14 and MobileNetV2-PANNs models exhibited remarkable accuracy, surpassing other CNN-based models with a score of over 0.85. To gain insights into the computational complexity of these baseline models, we analyzed their parameters. Surprisingly, the MobileNetV2-PANNs model, with a modest 1.9 million parameters, delivered competitive results, outperforming larger CNN models while maintaining a more compact size. In contrast, smaller models like MobileNetV1 and MobileNetV2, possessing 4.2 million and 3.5 million parameters, respectively, fell short when compared to the MobileNetV2-PANNs model, exhibiting a performance gap of 3%. Moreover, we found that the MobileNetV2-PANNs model has lower Floating Point Operations (FLOPs), making it an efficient model for aquaculture applications. In light of the recent advances in large-scale self-supervised pre-trained models, such as PANNs [24] and AST [58], which have substantially elevated audio classification performance on the AudioSet, we try to exploit their potential by fine-

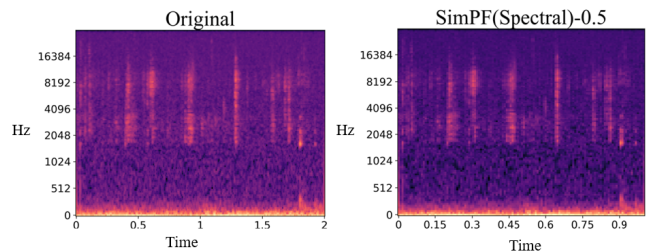


Fig. 4: Visualization of the impact of SimPFs on the mel-spectrogram of a FFIA audio clip with 50% compression factor

TABLE III: The results of the different audio-based methods on the different SNR conditions.

Model	-10 dB	-5 dB	0 dB	10 dB	20 dB
MobileNetV1	0.652	0.639	0.699	0.737	0.761
MobileNetV2	0.646	0.662	0.676	0.737	0.762
ResNet18	0.671	0.671	0.711	0.743	0.768
ResNet22	0.675	0.690	0.714	0.759	0.804
CNN10	0.691	0.701	0.713	0.761	0.807
CNN14	<b>0.704</b>	0.712	0.723	0.759	0.818
Pre-CNN6	0.662	0.656	0.683	0.710	0.787
Pre-CNN10	0.702	0.708	0.722	0.741	0.785
Pre-Mobilevit	0.623	0.623	0.695	0.727	0.776
<b>MobileNetV2-PANNs</b>	0.688	<b>0.718</b>	<b>0.726</b>	<b>0.763</b>	<b>0.826</b>

TABLE IV: The performance of different A-V fusion methods on AV-FFIA dataset and A-V fusion under noise environment.

Model	A only	V only	AV Fusion	-10 dB	-5 dB	0 dB	10 dB	20 dB
Self-attention	0.821	<b>0.883</b>	0.892	0.713	0.751	0.774	0.826	0.863
Cross-attention	n/a	n/a	<b>0.917</b>	<b>0.727</b>	0.768	0.805	0.834	0.867
MBT	n/a	n/a	0.724	0.617	0.631	0.652	0.681	0.713
U-FFIA	0.786	0.836	0.892	0.721	0.763	0.797	0.836	0.872
<b>U-FFIA + KD (Proposed)</b>	<b>0.824</b>	0.857	0.907	0.726	<b>0.779</b>	<b>0.806</b>	<b>0.835</b>	<b>0.876</b>

TABLE V: The FLOPs and parameters of different A-V fusion methods on the AV-FFIA dataset.

Model	FLOPs			Parameters		
	A (M)	V (G)	AV (G)	A (M)	V (M)	AV (M)
Self-attention	210.346	68.193	68.404	39.781	45.710	47.695
Cross-attention	n/a	n/a	60.933	n/a	n/a	35.082
MBT	n/a	n/a	68.690	n/a	n/a	47.689
<b>U-FFIA</b>	<b>105.336</b>	<b>15.401</b>	<b>15.488</b>	<b>21.032</b>	<b>19.506</b>	<b>21.626</b>

TABLE VI: Ablation study for modality dropout probabilities on U-FFIA.

PT			Modality	Clean	Noise				
$P_{av}$	$P_a$	$P_v$			-10 dB	-5 dB	0 dB	10 dB	20 dB
1	0	0	AV	<b>0.917</b>	0.798	0.819	0.826	0.864	0.887
0.7	0.15	0.15	AV	0.902	0.781	0.803	0.812	0.846	0.881
0.5	0.25	0.25	AV	0.895	0.726	0.779	0.806	0.832	0.872
0.4	0.2	0.4	AV	0.862	0.702	0.768	0.776	0.837	0.853
0.7	0.15	0.15	A	0.714	0.581	0.602	0.632	0.656	0.682
0.5	0.25	0.25	A	<b>0.786</b>	0.596	0.625	0.654	0.698	0.732
0.4	0.2	0.4	A	0.761	0.588	0.612	0.646	0.671	0.703
0.7	0.15	0.15	V	0.740	0.684	0.684	0.684	0.684	0.684
0.5	0.25	0.25	V	0.836	0.788	0.788	0.788	0.788	0.788
0.4	0.2	0.4	V	<b>0.858</b>	0.803	0.803	0.803	0.803	0.803

tuning them on our AV-FFIA dataset. The results indicated that pre-trained models are better than retrained models and CNN-based models surpassed transformer models on the AV-FFIA dataset. In contrast, the transformer models, originally designed for sequential data, such as natural language processing (NLP) tasks, heavily rely on self-attention mechanisms, which excel in modelling long-range dependencies but might struggle to discern fine-grained local patterns evident in audio spectrograms. Furthermore, we investigated the effectiveness of the SimPF (Spectral) method with varying compression coefficient settings on MobileNetV2 models. Encouragingly, even with a 50% compression setting, we observed only a negligible 0.01% decrease in classification accuracy and the number of FLOPs reduced by half to 66.979 M. Visual analysis in Fig. 4 revealed that despite reducing the spectrogram resolution by half, the fundamental patterns of fish feeding sounds remained intact. As a result, we adopted this method as an effective means to reduce redundant information within the mel-spectrogram.

### B. The benchmark results of video-based FFIA

We compared commonly used video classification models, including I3D [65], S3D [64], and 3D-ViT [63] models, on our AV-FFIA dataset. We randomly sampled 20 frames from the original 50 frames to reduce the large amount of redundant information in videos. Table II presents the performance of different video-based baseline models on the AV-FFIA dataset, with S3D models achieving the highest accuracy of 0.898, outperforming other models. Compared with the performance of the S3D models, the performance of 3D-ViT [63] and ViViT [62] models reached approximately 0.88 and 0.74, respectively. This discrepancy can be attributed to the limitations of ViT-based architectures in capturing temporal information, potential overfitting due to inadequate training data, and differences in model complexity and parameter efficiency. S3D models are specifically designed to capture spatiotemporal information in videos using 3D convolutions. Additionally, they are often pre-trained on large-scale video datasets like Kinetics, which encompass diverse and representative video clips. One notable advantage of S3D models is their ability

to strike a balance between computational complexity and model performance. As evident from their fewer parameters (7.9 million) and FLOPs (22.826G) compared to I3D [65] and 3D-ResNet [78] models, they are more efficient, making them a promising choice for applications in aquaculture.

### C. The benchmark results of audio-visual based FFIA

We compared various audio-visual fusion methods, such as cross-attention, self-attention, and MBT on the *AV-FFIA* dataset. In Table IV, we present the results of different baseline methods based on audio-visual modalities on *AV-FFIA*. Compared with the performance achieved with individual modalities, we observed that all the audio-visual fusion methods surpassed any single modality, which indicates that the multimodal approach significantly outperforms the single-modality based approaches. In addition, we found that the robustness of the audio-visual approach surpasses the single modality based approaches under the noisy environment. Notably, the self-attention method achieved an accuracy of 0.882, while the cross-attention method achieved 0.917. We believe that the cross-attention method enables the model to selectively focus on relevant information in both audio and visual modalities, whereas the self-attention method treats all information equally.

Consider the scenario of fish feeding, where the fish quickly consumes all the current feed, resulting in no sound being produced. However, the video still shows the fish highly aggregated and in a state of hunger. The cross-attention method allows the information from the audio modality to complement that from the visual modality in such cases. On the other hand, the Multimodal Bottleneck Transformer (MBT) method achieved a lower accuracy of only 0.724 compared to the cross-attention method. This could be attributed to attention bottlenecks that attend to each modality sequentially, leading to a failure to capture the complex relationships among modalities. Consequently, there may be information loss and a lack of direct interaction between modalities.

### D. The unified model

Table IV provides an in-depth analysis of our proposed model and several audio-visual fusion methods that are currently in use. Our *U-FFIA* model achieved an accuracy of 0.786 and 0.836 for audio and video single modalities, respectively, and an accuracy of 0.907 for audio-visual fusion. It's worth noting that the use of fewer audio and video frames can slightly degrade the performance. However, knowledge distillation can significantly improve the performance of *U-FFIA* across both audio and video modes. Through the application of the knowledge distillation approach, we observed marked improvements in both audio and visual performance (0.824 and 0.857, respectively). These enhancements place the individual modality based model on par with other audio-visual fusion methods, including Self-attention and Cross-attention, in terms of performance. Furthermore, we conducted a thorough analysis of computational complexity and model parameters across various models (refer to Table V). In comparison to a Transformer model employing all video frames,

our proposed model with fewer video frames demonstrates a remarkable reduction of 57% in parameters, accompanied by a substantial 77% decrease in FLOPs, while maintaining a negligible 3% dip in performance. This efficiency is mirrored in the audio domain, where our model showcases a 48% decrease in model size in terms of the number of parameters and a 50% reduction in FLOPs, but with a marginal performance variance. Importantly, our proposed unified model exhibits comparable performance on audio-visual fusion while concurrently reducing the number of parameters and FLOPs by 54% and 77%, respectively. This compelling evidence underscores the efficiency of our proposed model. Additionally, our proposed model has better robustness, as shown in Table IV. Our proposed *U-FFIA* model is a single model capable of processing different modalities and achieved good performance for *AV-FFIA*, in both effectiveness and robustness in various scenarios.

### E. Ablation studies

To gain a deeper understanding of the impact of modality dropout configurations on our *AV-FFIA* dataset during training, we consider four different modality dropout configurations. These configurations are represented by the probabilities of using both audio and video streams  $P_{av}$ , only the audio stream  $P_a$ , and only the video stream  $P_v$ , as shown in Table VI. The first configuration, denoted as  $(P_{av}, P_a, P_v) = (1.00, 0.00, 0.00)$ , corresponds to not employing any modality dropout. When training the *U-FFIA* model, we observed that increasing the value of  $P_{av}$  in models trained with modality dropout resulted in slightly worse performance on the visual-only and audio-only test sets. We attribute this outcome to an imbalance in the training data, leading to overfitting in the audio-visual modality but insufficient training in the single modalities.

In contrast, a slight increase in the probability within the video modality resulted in a slight improvement in video performance. This improvement can be attributed to the simple linear transformation undergone by the video modality's input, capturing shallow visual features. Furthermore, to reduce computational complexity, we randomly down-sampled the video, resulting in a reduced number of video frames. Consequently, achieving optimal performance may necessitate additional training iterations. For the audio modality, the high-dimensional features are extracted from pre-trained models, as a result, satisfactory performance could be achieved with fewer iterations. Nevertheless, all three modality configurations significantly outperformed models trained without modality dropout, showing the importance of modality dropout in training a single model for three distinct modalities.

## VIII. CONCLUSION AND FUTURE WORK

In this paper, we have presented *U-FFIA*, a novel unified mixed-modality based method for FFIA. The *U-FFIA* is a single model capable of processing audio, visual or audio-visual modalities for FFIA. We also introduced a large-scale audio-visual dataset for FFIA and conducted extensive benchmarking experiments involving audio, video, and audio-visual fusion techniques on our new dataset. The *U-FFIA* model can achieve

performance better than (or on par with) SOTA modality-specific FFIA models, especially under noisy environments. In addition, our proposed model achieved this level of performance while requiring significantly fewer computational resources, highlighting its efficiency and effectiveness for FFIA in aquaculture. In the future, we will expand the AV-FFIA dataset of different fish species and design on-device models to suit the needs of aquaculture applications.

## IX. ACKNOWLEDGMENT

This work was supported by the Research and demonstration of digital cage integrated monitoring system based on underwater robot [China grant 2022YFE0107100], Digital Fishery Cross-Innovative Talent Training Program of the China Scholarship Council (DF-Project) and a Research Scholarship from the China Scholarship Council. Ethics approval for this study was obtained from the Welfare and Ethical Committee of China Agricultural University (Ref: AW30901202-5-1). For the purpose of open access, the authors have applied a Creative Commons Attribution (CC BY) licence to any author-accepted manuscript version arising.

## REFERENCES

- [1] X. Yang, S. Zhang, J. Liu, Q. Gao, S. Dong, and C. Zhou, "Deep learning for smart fish farming: applications, opportunities and challenges," *Reviews in Aquaculture*, vol. 13, no. 1, pp. 66–90, 2021.
- [2] C. Wang, Z. Li, T. Wang, X. Xu, X. Zhang, and D. Li, "Intelligent fish farm—the future of aquaculture," *Aquaculture International*, pp. 1–31, 2021.
- [3] Y. Atoum, S. Srivastava, and X. Liu, "Automatic feeding control for dense aquaculture fish tanks," *IEEE Signal Processing Letters*, vol. 22, no. 8, pp. 1089–1093, 2014.
- [4] D. An, J. Huang, and Y. Wei, "A survey of fish behaviour quantification indexes and methods in aquaculture," *Reviews in Aquaculture*, vol. 13, no. 4, pp. 2169–2189, 2021.
- [5] L. Yang, Y. Chen, T. Shen, H. Yu, and D. Li, "A BlendMask-VoVNetV2 method for quantifying fish school feeding behavior in industrial aquaculture," *Computers and Electronics in Agriculture*, vol. 211, p. 108005, 2023.
- [6] C. Zhou, D. Xu, L. Chen, S. Zhang, C. Sun, X. Yang, and Y. Wang, "Evaluation of fish feeding intensity in aquaculture using a convolutional neural network and machine vision," *Aquaculture*, vol. 507, pp. 457–465, 2019.
- [7] Y. Zhang, C. Xu, R. Du, Q. Kong, D. Li, and C. Liu, "MSIF-MobileNetV3: An improved mobilenetv3 based on multi-scale information fusion for fish feeding behavior analysis," *Aquacultural Engineering*, vol. 102, p. 102338, 2023.
- [8] S. Feng, X. Yang, Y. Liu, Z. Zhao, J. Liu, Y. Yan, and C. Zhou, "Fish feeding intensity quantification using machine vision and a lightweight 3D ResNet-GloRe network," *Aquacultural Engineering*, vol. 98, p. 102244, 2022.
- [9] Q. Kong, R. Du, Q. Duan, Y. Zhang, Y. Chen, D. Li, C. Xu, W. Li, and C. Liu, "A recurrent network based on active learning for the assessment of fish feeding status," *Computers and Electronics in Agriculture*, vol. 198, p. 106979, 2022.
- [10] D. Li, Z. Wang, S. Wu, Z. Miao, L. Du, and Y. Duan, "Automatic recognition methods of fish feeding behavior in aquaculture: a review," *Aquaculture*, vol. 528, p. 735508, 2020.
- [11] L. Yang, H. Yu, Y. Cheng, S. Mei, Y. Duan, D. Li, and Y. Chen, "A dual attention network based on EfficientNet-B2 for short-term fish school feeding behavior analysis in aquaculture," *Computers and Electronics in Agriculture*, vol. 187, p. 106316, 2021.
- [12] X. Yu, Y. Wang, D. An, and Y. Wei, "Identification methodology of special behaviors for fish school based on spatial behavior characteristics," *Computers and Electronics in Agriculture*, vol. 185, p. 106169, 2021.
- [13] D. Wei, E. Bao, Y. Wen, S. Zhu, Z. Ye, and J. Zhao, "Behavioral spatial-temporal characteristics-based appetite assessment for fish school in recirculating aquaculture systems," *Aquaculture*, vol. 545, p. 737215, 2021.
- [14] N. Ubina, S. C. Cheng, C. C. Chang, and H. Y. Chen, "Evaluating fish feeding intensity in aquaculture with convolutional neural networks," *Aquacultural Engineering*, vol. 94, p. 102178, 2021.
- [15] J. Y. Su, P. H. Zhang, S. Y. Cai, S. C. Cheng, and C. C. Chang, "Visual analysis of fish feeding intensity for smart feeding in aquaculture using deep learning," in *International Workshop on Advanced Imaging Technology (IWAIT) 2020*, vol. 11515, pp. 94–99, SPIE, 2020.
- [16] H. Maaloy, A. Aamodt, and E. Misimi, "A spatio-temporal recurrent network for salmon feeding action recognition from underwater videos in aquaculture," *Computers and Electronics in Agriculture*, vol. 167, p. 105087, 2019.
- [17] C. Zhou, K. Lin, D. Xu, L. Chen, Q. Guo, C. Sun, and X. Yang, "Near infrared computer vision and neuro-fuzzy model-based feeding decision system for fish in aquaculture," *Computers and Electronics in Agriculture*, vol. 146, pp. 114–124, 2018.
- [18] L. Yang, Y. Liu, H. Yu, X. Fang, L. Song, D. Li, and Y. Chen, "Computer vision models in intelligent aquaculture with emphasis on fish detection and behavior analysis: a review," *Archives of Computational Methods in Engineering*, vol. 28, no. 4, pp. 2785–2816, 2021.
- [19] C. Zhou, B. Zhang, K. Lin, D. Xu, C. Chen, X. Yang, and C. Sun, "Near-infrared imaging to quantify the feeding behavior of fish in aquaculture," *Computers and Electronics in Agriculture*, vol. 135, pp. 233–241, 2017.
- [20] R. Gao, T. H. Oh, K. Grauman, and L. Torresani, "Listen to look: Action recognition by previewing audio," in *Proceedings of the IEEE/CVF Conference on Computer Vision and Pattern Recognition*, pp. 10457–10467, 2020.
- [21] Y. B. Lin, J. Lei, M. Bansal, and G. Bertasius, "Eclipse: Efficient long-range video retrieval using sight and sound," in *European Conference on Computer Vision*, pp. 413–430, Springer, 2022.
- [22] M. Cui, X. Liu, J. Zhao, J. Sun, G. Lian, T. Chen, M. D. Plumbley, D. Li, and W. Wang, "Fish feeding intensity assessment in aquaculture: A new audio dataset affia3k and a deep learning algorithm," in *2022 IEEE 32nd International Workshop on Machine Learning for Signal Processing (MLSP)*, pp. 1–6, IEEE, 2022.
- [23] X. Liu, H. Liu, Q. Kong, X. Mei, M. D. Plumbley, and W. Wang, "Simple pooling front-ends for efficient audio classification," in *ICASSP 2023-2023 IEEE International Conference on Acoustics, Speech and Signal Processing (ICASSP)*, pp. 1–5, IEEE, 2023.
- [24] Q. Kong, Y. Cao, T. Iqbal, Y. Wang, W. Wang, and M. D. Plumbley, "PANNs: Large-scale pretrained audio neural networks for audio pattern recognition," *IEEE/ACM Transactions on Audio, Speech, and Language Processing*, vol. 28, pp. 2880–2894, 2020.
- [25] G. Hinton, O. Vinyals, J. Dean, *et al.*, "Distilling the knowledge in a neural network," *arXiv:1503.02531*, vol. 2, no. 7, 2015.
- [26] J. Zhao, W. J. Bao, F. D. Zhang, Z. Y. Ye, Y. Liu, M. W. Shen, and S. M. Zhu, "Assessing appetite of the swimming fish based on spontaneous collective behaviors in a recirculating aquaculture system," *Aquacultural Engineering*, vol. 78, pp. 196–204, 2017.
- [27] M. Mathur, D. Vasudev, S. Sahoo, D. Jain, and N. Goel, "Crosspooled fishnet: transfer learning based fish species classification model," *Multimedia Tools and Applications*, vol. 79, pp. 31625–31643, 2020.
- [28] P. L. F. Albuquerque, V. Garcia, A. d. S. O. Junior, T. Lewandowski, C. Detweiler, A. B. Gonçalves, C. S. Costa, M. H. Naka, and H. Pistori, "Automatic live fingerlings counting using computer vision," *Computers and Electronics in Agriculture*, vol. 167, p. 105015, 2019.
- [29] S. Liu, X. Li, M. Gao, Y. Cai, R. Nian, P. Li, T. Yan, and A. Lendasse, "Embedded online fish detection and tracking system via yolov3 and parallel correlation filter," in *Oceans 2018 Mts/Ieee Charleston*, pp. 1–6, IEEE, 2018.
- [30] G. Wang, A. Muhammad, C. Liu, L. Du, and D. Li, "Automatic recognition of fish behavior with a fusion of rgb and optical flow data based on deep learning," *Animals*, vol. 11, no. 10, p. 2774, 2021.
- [31] R. FROESE, "Fishbase. world wide web electronic publication," <http://www.fishbase.org>, 2009.
- [32] A. N. Rice, S. C. Farina, A. J. Makowski, I. M. Kaatz, P. S. Lobel, W. E. Bemis, and A. H. Bass, "Evolutionary patterns in sound production across fishes," *Ichthyology and Herpetology*, vol. 110, no. 1, pp. 1–12, 2022.
- [33] M. Phillips, "The feeding sounds of rainbow trout, *salmo gairdneri* richardson," *Journal of Fish Biology*, vol. 35, no. 4, pp. 589–592, 1989.
- [34] Y. Yamaguchi, "Spectrum analysis of sounds made by feeding fish in relation to their movement," *Bull. Fac. Fish., Mie Univ.*, vol. 2, pp. 39–42, 1975.
- [35] E. Shishkova, "Notes and investigations on sound produced by fishes," *Tr. Vses. Inst. Ribn. Hozaist. Okeanograf*, vol. 280, p. 294, 1958.
- [36] A. Takemura, "The attraction effect of natural feeding sound in fish," *Bull. Fac. Fish. Nagasaki Univ.*, vol. 63, pp. 1–4, 1988.

- [37] R. Qi, H. Liu, and S. Liu, "Effects of different culture densities on the acoustic characteristics of micropterus salmoides feeding," *Fishes*, vol. 8, no. 3, p. 126, 2023.
- [38] Z. Du, M. Cui, Q. Wang, X. Liu, X. Xu, Z. Bai, C. Sun, B. Wang, S. Wang, and D. Li, "Feeding intensity assessment of aquaculture fish using mel spectrogram and deep learning algorithms," *Aquacultural Engineering*, p. 102345, 2023.
- [39] Y. Zeng, X. Yang, L. Pan, W. Zhu, D. Wang, Z. Zhao, J. Liu, C. Sun, and C. Zhou, "Fish school feeding behavior quantification using acoustic signal and improved swin transformer," *Computers and Electronics in Agriculture*, vol. 204, p. 107580, 2023.
- [40] R. Gao, R. Feris, and K. Grauman, "Learning to separate object sounds by watching unlabeled video," in *Proceedings of the European Conference on Computer Vision (ECCV)*, pp. 35–53, 2018.
- [41] R. Gao and K. Grauman, "2.5 d visual sound," in *Proceedings of the IEEE/CVF Conference on Computer Vision and Pattern Recognition*, pp. 324–333, 2019.
- [42] K. Choi, M. Kersner, J. Morton, and B. Chang, "Temporal knowledge distillation for on-device audio classification," in *ICASSP 2022-2022 IEEE International Conference on Acoustics, Speech and Signal Processing (ICASSP)*, pp. 486–490, IEEE, 2022.
- [43] S. Theodoridis and K. Koutroumbas, *Pattern recognition*. Elsevier, 2006.
- [44] Y. Wu, L. Zhu, Y. Yan, and Y. Yang, "Dual attention matching for audio-visual event localization," in *Proceedings of the IEEE/CVF international conference on computer vision*, pp. 6292–6300, 2019.
- [45] Y. B. Lin, Y. J. Li, and Y. C. F. Wang, "Dual-modality seq2seq network for audio-visual event localization," in *ICASSP 2019-2019 IEEE International Conference on Acoustics, Speech and Signal Processing (ICASSP)*, pp. 2002–2006, IEEE, 2019.
- [46] J. Li *et al.*, "Recent advances in end-to-end automatic speech recognition," *APSIPA Transactions on Signal and Information Processing*, vol. 11, no. 1, 2022.
- [47] P. Lucey and G. Potamianos, "Lipreading using profile versus frontal views," in *2006 IEEE Workshop on Multimedia Signal Processing*, pp. 24–28, IEEE, 2006.
- [48] F. Noroozi, M. Marjanovic, A. Njegus, S. Escalera, and G. Anbarjafari, "Audio-visual emotion recognition in video clips," *IEEE Transactions on Affective Computing*, vol. 10, no. 1, pp. 60–75, 2017.
- [49] M. S. Hossain and G. Muhammad, "Emotion recognition using deep learning approach from audio-visual emotional big data," *Information Fusion*, vol. 49, pp. 69–78, 2019.
- [50] M. Hagiwara, "Aves: Animal vocalization encoder based on self-supervision," *arXiv preprint arXiv:2210.14493*, 2022.
- [51] Y. R. Pandeya, B. Bhattarai, U. Afzaal, J.-B. Kim, and J. Lee, "A monophonic cow sound annotation tool using a semi-automatic method on audio/video data," *Livestock Science*, vol. 256, p. 104811, 2022.
- [52] N. Bold, C. Zhang, and T. Akashi, "Bird species classification with audio-visual data using cnn and multiple kernel learning," in *2019 International Conference on Cyberworlds (CW)*, pp. 85–88, IEEE, 2019.
- [53] R. Nathan, C. T. Monk, R. Arlinghaus, T. Adam, J. Alos, M. Assaf, H. Baktoft, C. E. Beardsworth, M. G. Bertram, A. I. Bijleveld, *et al.*, "Big-data approaches lead to an increased understanding of the ecology of animal movement," *Science*, vol. 375, no. 6582, p. eabg1780, 2022.
- [54] X. L. Ng, K. E. Ong, Q. Zheng, Y. Ni, S. Y. Yeo, and J. Liu, "Animal kingdom: A large and diverse dataset for animal behavior understanding," in *Proceedings of the IEEE/CVF Conference on Computer Vision and Pattern Recognition*, pp. 19023–19034, 2022.
- [55] J. Salamon, J. P. Bello, A. Farnsworth, and S. Kelling, "Fusing shallow and deep learning for bioacoustic bird species classification," in *IEEE International Conference on Acoustics, Speech and Signal Processing (ICASSP)*, pp. 141–145, 2017.
- [56] I. Kiskin, D. Zilli, Y. Li, M. Sinka, K. Willis, and S. Roberts, "Bioacoustic detection with wavelet-conditioned convolutional neural networks," *Neural Computing and Applications*, vol. 32, no. 4, pp. 915–927, 2020.
- [57] C. J. Huang, Y. J. Yang, D. X. Yang, and Y. J. Chen, "Frog classification using machine learning techniques," *Expert Systems with Applications*, vol. 36, no. 2, pp. 3737–3743, 2009.
- [58] Y. Gong, Y. A. Chung, and J. Glass, "AST: Audio spectrogram transformer," *arXiv preprint arXiv:2104.01778*, 2021.
- [59] J. F. Gemmeke, D. P. Ellis, D. Freedman, A. Jansen, W. Lawrence, R. C. Moore, M. Plakal, and M. Ritter, "Audio set: An ontology and human-labeled dataset for audio events," in *2017 IEEE international conference on acoustics, speech and signal processing (ICASSP)*, pp. 776–780, IEEE, 2017.
- [60] Y. Liu, J. Yuan, and Z. Tu, "Motion-driven visual tempo learning for video-based action recognition," *IEEE Transactions on Image Processing*, vol. 31, pp. 4104–4116, 2022.
- [61] A. V. Savchenko, "Video-based frame-level facial analysis of affective behavior on mobile devices using efficientnets," in *Proceedings of the IEEE/CVF Conference on Computer Vision and Pattern Recognition*, pp. 2359–2366, 2022.
- [62] A. Arnab, M. Dehghani, G. Heigold, C. Sun, M. Lucic, and C. Schmid, "Vivit: A video vision transformer," in *Proceedings of the IEEE/CVF international conference on computer vision*, pp. 6836–6846, 2021.
- [63] G. Bertasius, H. Wang, and L. Torresani, "Is space-time attention all you need for video understanding?," in *ICML*, vol. 2, p. 4, 2021.
- [64] S. Xie, C. Sun, J. Huang, Z. Tu, and K. Murphy, "Rethinking spatiotemporal feature learning: Speed-accuracy trade-offs in video classification," in *Proceedings of the European conference on computer vision (ECCV)*, pp. 305–321, 2018.
- [65] J. Carreira and A. Zisserman, "Quo vadis, action recognition? a new model and the kinetics dataset," in *proceedings of the IEEE Conference on Computer Vision and Pattern Recognition*, pp. 6299–6308, 2017.
- [66] A. Vaswani, N. Shazeer, N. Parmar, J. Uszkoreit, L. Jones, A. N. Gomez, L. Kaiser, and I. Polosukhin, "Attention is all you need," *Advances in neural information processing systems*, vol. 30, 2017.
- [67] A. Dosovitskiy, L. Beyer, A. Kolesnikov, D. Weissenborn, X. Zhai, T. Unterthiner, M. Dehghani, M. Minderer, G. Heigold, S. Gelly, *et al.*, "An image is worth 16x16 words: Transformers for image recognition at scale," *arXiv preprint arXiv:2010.11929*, 2020.
- [68] A. Nagrani, S. Yang, A. Arnab, A. Jansen, C. Schmid, and C. Sun, "Attention bottlenecks for multimodal fusion," *Advances in Neural Information Processing Systems*, vol. 34, pp. 14200–14213, 2021.
- [69] Y. Gong, A. H. Liu, A. Rouditchenko, and J. Glass, "UAVM: Towards unifying audio and visual models," *IEEE Signal Processing Letters*, vol. 29, pp. 2437–2441, 2022.
- [70] W. N. Hsu and B. Shi, "u-HuBERT: Unified mixed-modal speech pretraining and zero-shot transfer to unlabeled modality," in *Advances in Neural Information Processing Systems*, 2022.
- [71] O. Cayli, X. Liu, V. Kiliç, and W. Wang, "Knowledge distillation for efficient audio-visual video captioning," *arXiv preprint arXiv:2306.09947*, 2023.
- [72] X. Liu, Q. Huang, X. Mei, H. Liu, Q. Kong, J. Sun, S. Li, T. Ko, Y. Zhang, L. H. Tang, *et al.*, "Visually-aware audio captioning with adaptive audio-visual attention," *arXiv preprint arXiv:2210.16428*, 2022.
- [73] B. Shi, W. N. Hsu, K. Lakhota, and A. Mohamed, "Learning audio-visual speech representation by masked multimodal cluster prediction," *arXiv preprint arXiv:2201.02184*, 2022.
- [74] P. Chen, S. Liu, H. Zhao, and J. Jia, "Distilling knowledge via knowledge review," in *Proceedings of the IEEE/CVF Conference on Computer Vision and Pattern Recognition*, pp. 5008–5017, 2021.
- [75] D. S. Park, W. Chan, Y. Zhang, C. C. Chiu, B. Zoph, E. D. Cubuk, and Q. V. Le, "SpecAugment: A simple data augmentation method for automatic speech recognition," *arXiv:1904.08779*, 2019.
- [76] J. Kolarevic, O. Aas Hansen, A. Espmark, G. Baeverfjord, B. F. Terjesen, and B. Damsgard, "The use of acoustic acceleration transmitter tags for monitoring of atlantic salmon swimming activity in recirculating aquaculture systems (RAS)," *Aquacultural Engineering*, vol. 72, pp. 30–39, 2016.
- [77] D. P. Kingma and J. Ba, "Adam: A method for stochastic optimization," *arXiv:1412.6980*, 2014.
- [78] K. Hara, H. Kataoka, and Y. Satoh, "Learning spatio-temporal features with 3d residual networks for action recognition," in *Proceedings of the IEEE international conference on computer vision workshops*, pp. 3154–3160, 2017.